Earth and Planetary Science Letters 518 (2019) 127–135

Contents lists available at ScienceDirect

Earth and Planetary Science Letters

www.elsevier.com/locate/epsl

Abrupt mid-Holocene ice loss in the western Weddell Sea Embayment of Antarctica

Joanne S. Johnson [a,*], Keir A. Nichols [b], Brent M. Goehring [b], Greg Balco [c], Joerg M. Schaefer [d]

[a] British Antarctic Survey, High Cross, Madingley Road, Cambridge CB3 0ET, UK
[b] Department of Earth & Environmental Sciences, Tulane University, New Orleans, LA 70118, USA
[c] Berkeley Geochronology Center, 2455 Ridge Road, Berkeley, CA 94709, USA
[d] Lamont-Doherty Earth Observatory, Columbia University, Route 9W, Palisades, New York, NY 10964, USA

ARTICLE INFO

Article history:
Received 8 January 2019
Received in revised form 22 March 2019
Accepted 1 May 2019
Available online xxxx
Editor: J.-P. Avouac

Keywords:
Holocene
Antarctica
Weddell Sea
ice sheet
cosmogenic dating
in situ ^{14}C

ABSTRACT

The glacial history of the westernmost Weddell Sea sector of Antarctica since the Last Glacial Maximum is virtually unknown, and yet it has been identified as critical for improving reliability of glacio-isostatic adjustment models that are required to correct satellite-derived estimates of ice sheet mass balance. Better knowledge of the glacial history of this region is also important for validating ice sheet models that are used to predict future contribution of the Antarctic ice sheet to sea level rise. Here we present a new Holocene deglacial chronology from a site on the Lassiter Coast of the Antarctic Peninsula, which is situated in the western Weddell Sea sector. Samples from 12 erratic cobbles and 18 bedrock surfaces from a series of presently-exposed ridges were analysed for cosmogenic ^{10}Be exposure dating, and a smaller suite of 7 bedrock samples for in situ ^{14}C dating. The resulting ^{10}Be ages are predominantly in the range 80–690 ka, whereas bedrock yielded much younger in situ ^{14}C ages, in the range 6.0–7.5 ka for samples collected from 138–385 m above the modern ice surface. From these we infer that the ice sheet experienced a period of abrupt thinning over a short time interval (no more than 2700 years) in the mid-Holocene, resulting in lowering of its surface by at least 250 m. Any late Holocene change in ice sheet thickness — such as re-advance, postulated by several modelling studies — must lie below the present ice sheet surface. The substantial difference in exposure ages derived from ^{10}Be and ^{14}C dating for the same samples additionally implies ubiquitous ^{10}Be inheritance acquired during ice-free periods prior to the last deglaciation, an interpretation that is consistent with our glacial-geomorphological field observations for former cold-based ice cover. The results of this study provide evidence for an episode of abrupt ice sheet surface lowering in the mid-Holocene, similar in rate, timing and magnitude to at least two other locations in Antarctica.

1. Introduction

Ice streams flowing into the Weddell Sea Embayment (WSE) of Antarctica at the present day drain approximately a fifth of the Antarctic Ice sheet (Joughin et al., 2006). Modelling studies suggest that changes in the current patterns of ocean circulation in the region over the next centuries could bring warm ocean water into contact with grounding lines, resulting in increasing contributions to sea level rise from this sector of the ice sheet (e.g. Hellmer et al., 2012; Wright et al., 2014; Ritz et al., 2015). It is therefore critical to develop a realistic understanding of how the drainage basins surrounding the WSE are likely to respond to future environmental change. Physical models that simulate such changes require glacial-geological evidence for past ice sheet behaviour for their validation (DeConto and Pollard, 2016). As a result of several marine and terrestrial geological campaigns studying the eastern and central regions of the WSE during the past decade — summarised in Hillenbrand et al., 2014, and subsequently Arndt et al., 2017; Balco et al., 2017; Bentley et al., 2017; Fogwill et al., 2014; Hein et al., 2014, 2016 — understanding of the configuration and extent of the Antarctic ice sheet in the WSE during the Last Glacial Maximum (LGM), as well as its subsequent thinning and retreat, has significantly increased. However, the westernmost margin of the WSE has seldom been visited; thus the pace and pattern of ice sheet change there since the LGM remains virtually unknown.

* Corresponding author.
E-mail address: jsj@bas.ac.uk (J.S. Johnson).

https://doi.org/10.1016/j.epsl.2019.05.002

This data gap is limiting the development of models, particularly those that require knowledge of ice mass loading during the past 5,000 years in order to reliably model glacio-isostatic adjustment (GIA) (Whitehouse et al., 2012). In particular, the Lassiter Coast of the south-western WSE (Fig. 1a) has been identified as an area where satellite-derived estimates of ice sheet mass balance are at present extremely unreliable due to the lack of knowledge of the degree and timing of Holocene ice mass loss (Wolstencroft et al., 2015). The importance of determining Holocene history of the ice sheet occupying the WSE has been further highlighted by several recent modelling studies which suggest that it may have been more dynamic during the last 10,000 years than previously-thought: some simulations show a grounding line re-advance instead of progressive retreat to the present-day (Pollard et al., 2016, 2017; Golledge et al., 2014; Maris et al., 2015; Kingslake et al., 2018). Furthermore, Bradley et al. (2015) achieved a better fit to GPS observations of crustal uplift across the whole WSE in their ice loading simulations by invoking an extended period of retreat or thinning during the mid-Holocene, followed by a late Holocene re-advance. This paper presents geomorphological evidence for a formerly thicker ice sheet in the westernmost WSE than at present, and geochronological data (^{10}Be and in situ ^{14}C exposure ages) that provide constraints on the deglacial history of the ice sheet in that area during the Holocene.

2. Ice sheet configuration since the Last Glacial Maximum

Results of several terrestrial geomorphological and cosmogenic dating studies in the eastern and southern WSE have been interpreted as evidence that the ice sheet was no more than a few hundred metres thicker at the LGM than it is today (Bentley et al., 2010; Fogwill et al., 2004, 2014; Hein et al., 2011, 2014; Hodgson et al., 2012). Some also document periods of thinning through the early-mid Holocene in the southern region in the Ellsworth and Pensacola Mountains (Bentley et al., 2017; Hein et al., 2016; Balco et al., 2017). However, the deglacial history — both at LGM and Holocene — of the ice sheet in the westernmost WSE is, in contrast, virtually unknown because there has been only one terrestrial reconnaissance-scale glacial-geomorphological study in the region (Bentley et al., 2006) and only one research cruise has collected marine sediment cores from the western Ronne Ice Shelf front (*RV* Polarstern ANT-IV/3; Fütterer et al., 1987). Geophysical surveys from that cruise revealed pristine mega-scale glacial lineations preserved in sediment on the inner shelf of Ronne Trough (Stolldorf et al., 2012), implying that ice was grounded there during the late Pleistocene (Hillenbrand et al., 2014). The only published age constraint on grounded ice retreat from Ronne Trough — 5.3 ± 0.3 cal kyr BP, determined by radiocarbon dating of a glaciomarine diamicton in marine sediment (Hedges et al., 1995) — is a minimum limiting age and therefore does not preclude earlier retreat of grounded ice from the core site (Crawford et al., 1996).

The only terrestrial geomorphological study of the south-eastern Antarctic Peninsula determined cosmogenic ^{10}Be and ^{26}Al exposure ages for erratic cobbles collected from peaks situated within 30–50 km of the modern grounding line in the SE Antarctic Peninsula: Ferguson Nunataks and Mt Dewe (Fig. 1a; Bentley et al., 2006). These cobbles — transported to the sites by glaciers and subsequently exposed during ice sheet thinning — yielded a range of ages from 30 ka to 1.3 Ma, all suggesting that they experienced multiple periods of exposure since the LGM. Thus the authors were unable to constrain the onset of the last retreat of the Antarctic Peninsula ice sheet in the south-western WSE or to determine its trajectory through the Holocene. However, three erratics from the Behrendt Mountains in the central southern Antarctic Peninsula yielded Holocene exposure ages (7.2–12.3 ka; Bentley et al., 2006), suggesting that ice there was <300 m thicker than present by the early Holocene. Since the lowest sample analysed was situated 250 m above the present ice sheet surface, their exposure age data do not preclude further ice sheet surface lowering after 7.2 ka.

Since publication of the Bentley et al. (2006) study, the in situ-produced nuclide ^{14}C has become more frequently utilised for glacio-geological studies in Antarctica, although only a few studies have reported more than a handful of in situ ^{14}C ages. The nuclide has a half-life short enough that it decays rapidly during ice cover and hence permits determination of Holocene ice mass loss without the problem of nuclide inheritance that often complicates interpretation of ^{10}Be and ^{26}Al exposure age data in areas where there has been a lack of ice-sheet erosion. The present study takes advantage of this, demonstrating with 7 in situ ^{14}C ages its importance for determining reliable Holocene deglacial histories in areas of Antarctica where ^{10}Be inheritance is ubiquitous.

3. Study area and methods

We present exposure age data from a suite of rock samples collected from currently-exposed peaks and ridges of the Bowman and Smith Peninsulas on the Lassiter Coast of Antarctica (Fig. 1b). Several major outlet glaciers dissect the region at the present day, draining ice from the Antarctic Peninsula into the western and south-western WSE. The study sites were chosen for their close proximity to the modern grounding line (Fig. 1), where the greatest ice sheet thickness change since the LGM is expected. Details of sample collection and field methods are provided in Supplementary Data, Appendix I. Sparsely-distributed erratic cobbles of local lithology with sub-angular shape (Fig. 2a), juxtaposed with relatively-smooth bedrock surfaces and occasional tors (Fig. 2b and 2c), provide evidence for past ice cover. Small accumulations of till in bedrock hollows also confirm former ice cover. Bedrock in the region consists of extensive granodiorite and quartz diorite of the Lassiter Coast Intrusive Suite, co-existing with Latady Formation metasediments (Vennum and Rowley, 1986) and minor exposures of hornblende-rich pegmatites. Only the granodiorite and quartz diorite lithologies are suitable for exposure dating; however, all erratics observed in the study area were of this lithology.

In total, we collected 74 samples from bedrock and erratic cobbles from ice-free peaks adjacent to Johnston Glacier. Of these, we selected 36 for exposure dating as follows: 18 bedrock samples and 12 erratics — including some pairs from the same elevation — from exposed ridges at four nunataks on the central Bowman Peninsula (Mt Lampert and three un-named peaks; Fig. 1b), and six additional samples — 2 bedrock and 6 erratics — from Mt Owen, Mt Rath and Mt Light (Fig. 1b). All sites are situated within 15 km of the present grounding line. Samples were collected from a range of altitudes between 510–1141 m asl (Table 1), equating to 20–651 m above the modern ice sheet surface at 490 m asl (see Supplementary material, Appendix I, section 1.2). Fresh unweathered samples were selected where possible, and pitted and spalled erratics were avoided to minimise both the effect of post-depositional geomorphic processes and the likelihood of cosmogenic nuclide inheritance from exposure prior to the LGM (which is common in Antarctica; Balco, 2011).

Cosmogenic ^{10}Be exposure ages were determined on both erratic cobbles and bedrock from all study sites. In situ cosmogenic ^{14}C was measured in 7 bedrock samples from the central Bowman Peninsula; these samples were selected because they span a wide altitudinal range and thus their ^{14}C exposure ages would provide a check on the timing and magnitude of deglaciation derived from ^{10}Be dating. Since it is conceivable (although unlikely) that sample sites might not have been ice-covered during the LGM for long enough for all the ^{14}C accumulated during prior

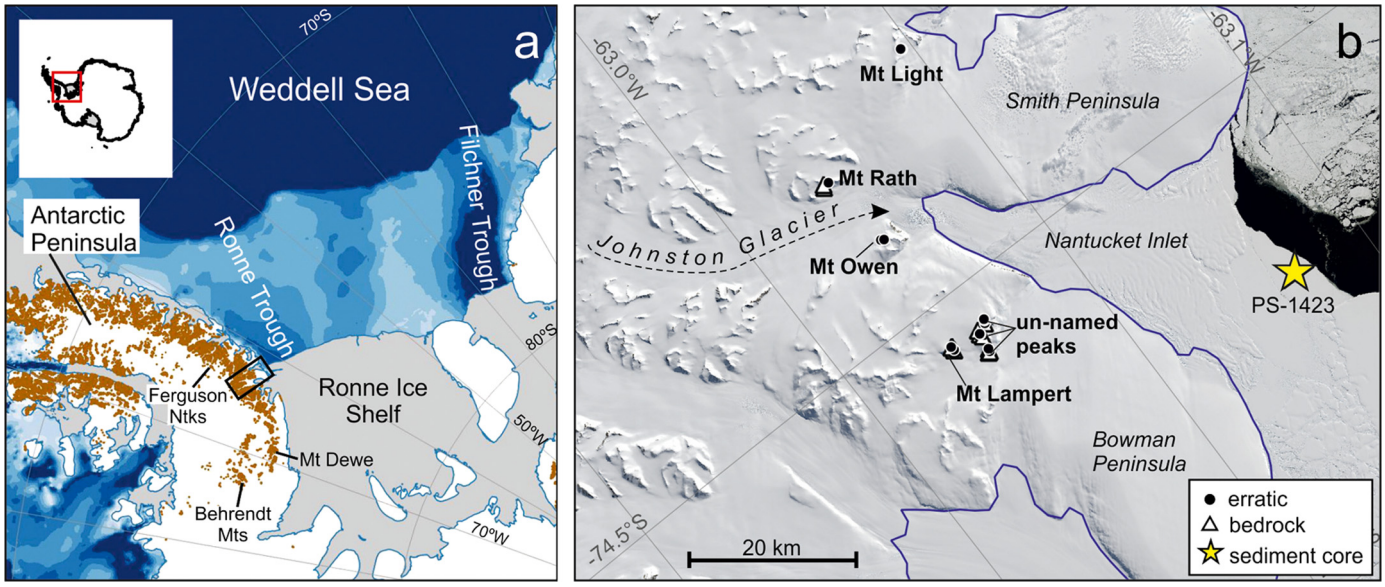

Fig. 1. Location of study area. (a) Map of the Antarctic Peninsula and westernmost Weddell Sea Embayment, showing location of study area on Lassiter Coast (black rectangle). Inset shows area covered by main map. Also shown are the locations of key sites mentioned in the text. (b) Map of study area located within black rectangle in panel a. The Landsat-8 image (© 2018 DigitalGlobe, Inc.) is provided courtesy of U.S. Geological Survey; the blue line is the 2011 grounding line (Rignot et al., 2011). Locations of samples analysed in this study are indicated by solid and open symbols as shown in legend, and sample site names are shown in bold). The star marks the location of marine sediment core, PS-1423 (see text). (For interpretation of the colours in the figure(s), the reader is referred to the web version of this article.)

Table 1
Sample details and location information.

Sample ID	Location	Type	Latitude	Longitude	Altitude (m a.s.l.)	Shielding factor
P11.6.3	Bowman Peninsula	bedrock	−74.5475	−62.4297	850	1.000
P11.11.2	Bowman Peninsula	bedrock	−74.5714	−62.4789	675	1.000
P11.11.4	Bowman Peninsula	bedrock	−74.5735	−62.4808	628	0.997
P11.11.6	Bowman Peninsula	bedrock	−74.5740	−62.4817	607	0.999
P11.12.1	Bowman Peninsula	bedrock	−74.5570	−62.4676	800	1.000
P11.12.2	Bowman Peninsula	bedrock	−74.5551	−62.4692	830	1.000
P11.12.3	Bowman Peninsula	bedrock	−74.5535	−62.4703	868	1.000
P11.12.4	Bowman Peninsula	bedrock	−74.5536	−62.4702	864	1.000
P11.12.6	Bowman Peninsula	bedrock	−74.5532	−62.4720	875	1.000
P11.13.2	Bowman Peninsula (Mt Lampert)	bedrock	−74.5499	−62.5906	690	0.998
P11.13.3	Bowman Peninsula (Mt Lampert)	bedrock	−74.5489	−62.5897	710	0.977
P11.13.5	Bowman Peninsula (Mt Lampert)	bedrock	−74.5465	−62.5919	768	0.998
P11.13.6	Bowman Peninsula (Mt Lampert)	bedrock	−74.5457	−62.5934	795	1.000
P11.13.9	Bowman Peninsula (Mt Lampert)	bedrock	−74.5503	−62.5909	663	0.997
P11.14.1	Bowman Peninsula	bedrock	−74.5745	−62.4881	510	0.977
P11.14.2	Bowman Peninsula	bedrock	−74.5741	−62.4840	585	0.994
P11.14.4	Bowman Peninsula	bedrock	−74.5740	−62.4841	589	0.994
P11.14.5	Bowman Peninsula	bedrock	−74.5742	−62.4831	593	0.994
P11.6.4	Bowman Peninsula	erratic	−74.5475	−62.4297	850	1.000
P11.6.6	Bowman Peninsula	erratic	−74.5447	−62.4236	822	1.000
P11.6.7A	Bowman Peninsula	erratic	−74.5434	−62.4229	798	0.998
P11.6.7B	Bowman Peninsula	erratic	−74.5434	−62.4229	798	0.998
P11.8.1	Bowman Peninsula	erratic	−74.5533	−62.4706	875	1.000
P11.8.3	Bowman Peninsula	erratic	−74.5530	−62.4716	873	0.999
P11.11.3	Bowman Peninsula	erratic	−74.5710	−62.4797	671	1.000
P11.11.5	Bowman Peninsula	erratic	−74.5740	−62.4817	607	0.999
P11.12.5	Bowman Peninsula	erratic	−74.5536	−62.4702	864	0.996
P11.13.1	Bowman Peninsula (Mt Lampert)	erratic	−74.5499	−62.5906	690	0.999
P11.13.7	Bowman Peninsula (Mt Lampert)	erratic	−74.5457	−62.5934	795	0.981
P11.13.8	Bowman Peninsula (Mt Lampert)	erratic	−74.5457	−62.5934	795	1.000
P11.15.5	Mt Rath	bedrock	−74.3280	−62.6028	1104	1.000
P11.15.7	Mt Rath	bedrock	−74.3307	−62.6078	1055	1.000
P11.15.3	Mt Rath	erratic	−74.3293	−62.5825	1141	0.987
P11.17.4	Mt Light	erratic	−74.2646	−62.0396	909	1.000
P11.17.5	Mt Light	erratic	−74.2637	−62.0416	937	1.000
P11.17.6	Mt Light	erratic	−74.2635	−62.0431	952	0.999
P11.10.1	Mt Owen	erratic	−74.4109	−62.5562	848	0.989
P11.10.9	Mt Owen	erratic	−74.4126	−62.5451	932	1.000

Fig. 2. Surface features on nunataks of the Bowman Peninsula, Lassiter Coast. (a) Sub-angular granodiorite erratic cobbles — indicated by arrows — perched on smooth bedrock surfaces of the same lithology. Compass and pen for scale. Photograph location: −74.5027°S/−62.5664°W (b) Bedrock surface with abundant weathering pits. Smith Peninsula (situated NE of Bowman Peninsula; Fig. 1b) is visible in the background. Person for scale. Location: −74.5434°S/−62.4229°W (c) Small tor-like feature — marked with an arrow — with weathering pits on its uppermost surface, formed in granodiorite bedrock. Person for scale. Location: −74.5535°S/−62.4703°W.

exposure to decay, the bedrock ^{14}C ages should be considered as maximum ages for deglaciation of the sample sites. For determining the exposure history of a site since the last glacial period using in situ ^{14}C, it should not make any difference whether bedrock or erratics are analysed because, unlike ^{10}Be, ^{14}C from exposure prior to the LGM decays rapidly rather than remaining in the rock surface (e.g. Briner et al., 2014; Johnson et al., 2017; Young et al., 2018). Although there will always be some residual ^{14}C (approximately 5% in a surface that was ice-covered at 25 ka, for example), the ^{14}C measured is predominantly that which accumulated in the rock surface only since the LGM. However, in contrast to erratics which could have been transported from elsewhere during the LGM, there is zero chance that bedrock could have moved since it was last covered by ice; therefore, any ^{14}C age versus altitudinal profile on bedrock samples is likely to more-reliably reflect the trajectory of post-LGM ice sheet change. For this reason, bedrock samples were preferred for the in situ ^{14}C analysis in this study.

Samples were prepared for ^{10}Be measurement at Lamont-Doherty Earth Observatory cosmogenic nuclide laboratory, and analysed at the Center for Accelerator Mass Spectrometry, Lawrence Livermore National Laboratory, USA; quartz for in situ ^{14}C analysis was isolated at Tulane University Cosmogenic Nuclide Laboratory, USA, and the extracted carbon and stable carbon isotope ratios measured at Woods Hole National Ocean Sciences Accelerator Mass Spectrometry (NOSAMS) and UC Davis Stable Isotope Facility, respectively. Details of all samples, field methods, analytical procedures, exposure age calculations and analytical data are provided in Table 1 and Supplementary material Appendix I (Tables 2–3); analytical data are also publicly accessible in the ICE-D:Antarctica database (http://antarctica.ice-d.org).

4. Results

Bedrock from both the central Bowman Peninsula and Mts Owen, Rath and Light yielded ^{10}Be ages in the range 90–489 ka for elevations of 20–385 m above the modern ice surface, and erratic cobbles yielded ages of 19–686 ka for elevations above modern ice of 117–651 m (Fig. 3a). With just three exceptions, all the ages are older than 100 ka, significantly pre-dating the LGM. Whilst bedrock ages show a general trend of decreasing age with elevation (Fig. 3b), the erratic ^{10}Be ages are scattered with no apparent trend (Fig. 3a). In contrast, in situ ^{14}C measurement of selected bedrock samples from three closely-spaced nunataks of the central Bowman Peninsula (Mt Lampert and two un-named peaks; Fig. 1b) — including the highest sample collected — yielded ages in the much narrower range of 6.0 ± 0.5 to 7.5 ± 0.7 ka (Fig. 4) for elevations of 138–385 m above the modern ice surface. Since all the ^{14}C ages are Holocene (i.e. $<$11.7 ka), they provide evidence that all the bedrock samples analysed contain some ^{10}Be inherited from exposure prior to the LGM and thus their ^{10}Be ages cannot be interpreted as deglaciation ages. Combined with an almost complete absence of both erratics of exotic lithology (i.e. non-granodiorite) and striated bedrock surfaces across the study area, the presence of inherited ^{10}Be in all bedrock samples furthermore implies little erosion during glacial cycles. Such a situation is consistent with intermittent cover by cold-based (non-erosive) ice prior to the Holocene (Stone et al., 2003; Sugden et al., 2005).

We interpret the ^{14}C ages as reflecting the timing of thinning of Johnston Glacier, one of several large glaciers along the Lassiter Coast that drain ice from the eastern Antarctic Peninsula into the WSE (Fig. 1). Whilst the possibility that they reflect retreat of a local ice dome or cold-based glacier cannot be ruled out, no field evidence consistent with the former presence of local ice was observed in the study area. For example, no moraines or radial patterns of striations were seen, and some erratics have facetted surfaces, implying subglacial transport. In addition, the nunataks are not flat-topped and thus would not readily support small local ice domes. The ^{14}C ages imply that the ice sheet thinned in this

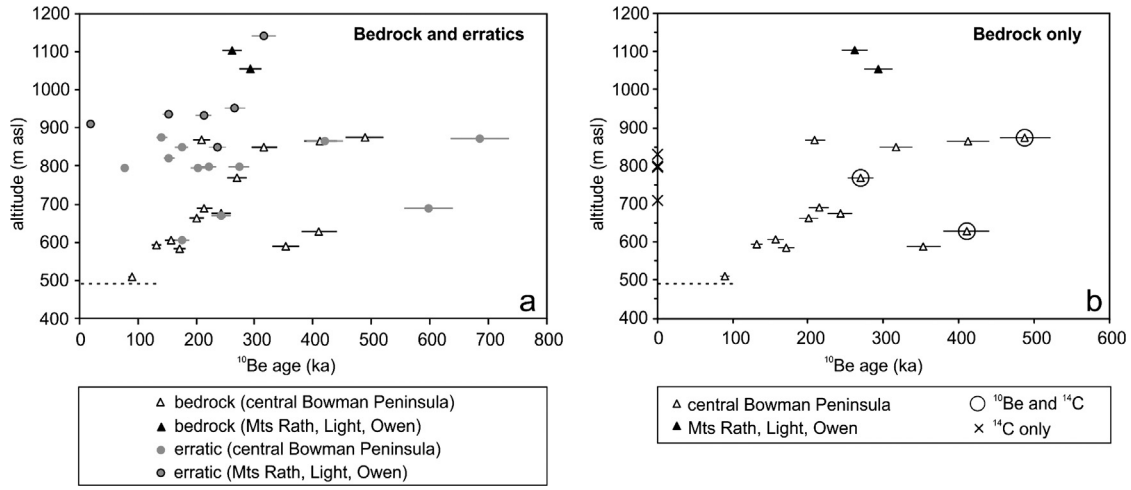

Fig. 3. ^{10}Be ages for samples collected from the central Bowman Peninsula and Mts Rath, Owen and Light. (a) ^{10}Be ages for bedrock and erratics. (b) Bedrock ^{10}Be ages in relation to the modern ice surface (horizontal dotted line). Circled samples denote those for which in situ ^{14}C was also measured; the crosses show the altitudes of 4 bedrock samples that were only analysed for in situ ^{14}C. For details of age calculations, see Supplementary material, Appendix I.

region by at least 250 m during a short interval of no more than 2700 years, between 6.0 ± 0.5 and 7.5 ± 0.7 ka. All the ^{14}C ages overlap within error, so we use the average age of those samples (6.9 ± 0.5 ka; Fig. 4) as the best estimate for when the ice surface had lowered to its modern elevation; however since there are no ages for elevations lower than 138 m above the modern ice surface, a lower rate of thinning proceeding into the later Holocene cannot be excluded.

5. Discussion

5.1. Extent and timing of deglaciation

The concurrence of ^{14}C ages from nunataks on the Bowman Peninsula is strong evidence that those peaks deglaciated during the mid-Holocene. The consistency of those ages furthermore implies rapid deglaciation, with at least 250 m of thinning occurring over just a few thousand years between 6.0 ± 0.5 and 7.5 ± 0.7 ka. Given that the highest elevation sample from which a reliable deglaciation (^{14}C) age was obtained is 385 m above the modern ice sheet surface, we infer that the ice sheet in this region was at least 385 m thicker than present at the LGM, and probably much thicker (the samples analysed were not collected from sufficiently high above the modern ice sheet surface to permit an estimation of maximum LGM ice thickness; a few quartz-bearing samples were collected from higher elevations further inland at Mt Rath, but were not analysed for in situ ^{14}C due to limited resources available for this project) (Fig. 5). In comparison with the nearest existing glacial-geomorphological constraints on ice sheet thickness – that suggest ice in the Behrendt Mountains was <300 m thicker than present by 7.2 ka (Bentley et al., 2006) – the new data imply that the ice sheet was ~100 m thicker on the WSE coast than at the Behrendt Mountains at that time (the highest sample analysed for ^{14}C, P11.12.6, yielded a deglaciation age of 6.7 ± 0.6 ka from 385 m above modern ice).

The ^{14}C exposure age data presented here also provide constraints on the timing of lowering of the ice sheet surface close to its modern elevation. Using the average of the upper seven in situ ^{14}C ages as the most likely timing for lowering of the ice sheet surface to its modern elevation implies that the ice sheet surface was close to present by 6.9 ka (Fig. 4). However, the data do not preclude thinning after 6.9 ka, perhaps even into the late Holocene, as is suggested by mismatches between GIA models and observed

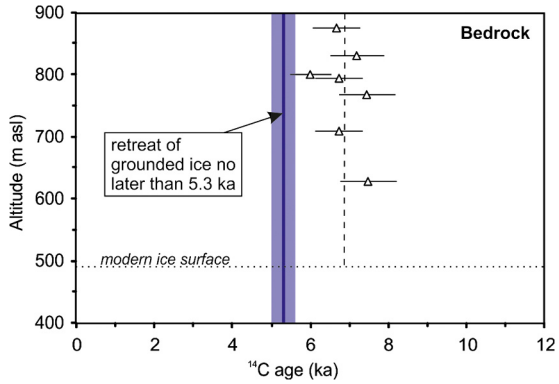

Fig. 4. In situ ^{14}C ages versus altitude for the bedrock samples encircled and shown as crosses in Fig. 3b; all are from the central Bowman Peninsula (Mt Lampert and two un-named peaks; Fig. 1b). Error bars show total measurement uncertainty estimated from the average scatter of replicate measurements (see Supplementary material, Table 3). The dashed vertical line is drawn at the average age of the samples (6.9 ka). The blue line represents a minimum age, with 2 sigma error shaded (Hedges et al., 1995), for grounded ice retreat derived from radiocarbon dating of marine sediment core PS-1423, which was collected 40 km ESE of our study area (Fig. 1b).

uplift (see section 5.3); nevertheless, any evidence for this must lie below the modern ice sheet surface and can only be accessed by subglacial bedrock drilling (see Spector et al., 2018).

At several other sites on the eastern Antarctic Peninsula, Bentley et al. (2006) reported a large proportion of samples showing evidence for ^{10}Be and ^{21}Al inheritance, which they attributed to cover by cold-based ice. ^{10}Be ages from the Lassiter Coast samples are all considerably older than the ^{14}C ages, and are all >80 kyrs older than LGM. Thus they must contain a large amount of inherited ^{10}Be. We interpret this as evidence for lack of erosion during multiple periods of cover by cold-based ice. This interpretation is further supported by the geomorphological observations described in section 3, such as the presence of few erratics of only local lithologies, as well as landscape features such as tors and weathering pits that can survive several periods of glaciation under conditions of minimal erosion (Sugden et al., 2005). Evidence for cover by cold-based ice is widespread around the WSE (e.g. Balco et al., 2017; Bentley et al., 2017; Hein et al., 2014).

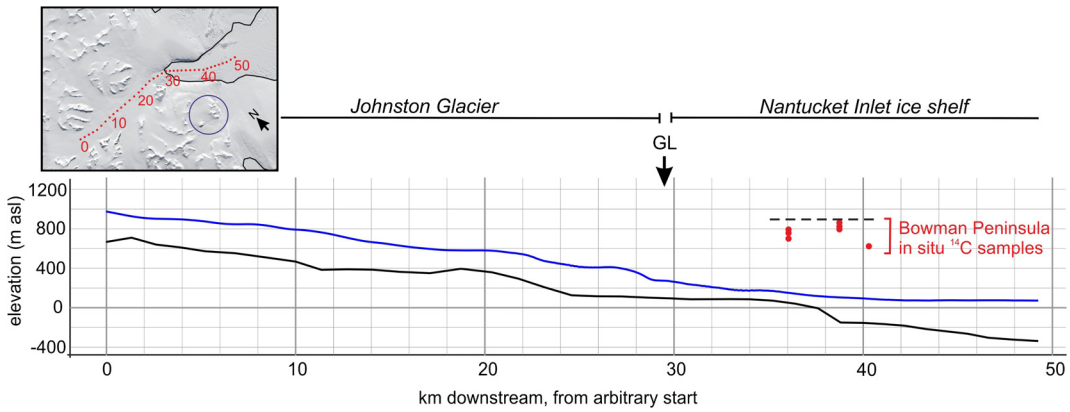

Fig. 5. Mid-Holocene ice thickness of Johnston Glacier — inferred from in situ ^{14}C exposure ages — compared with the modern configuration. Inset: Location of a profile along the flowline of Johnston Glacier, with distance downstream in km from an arbitrary starting position. The profile is shown in cross-section below. The blue circle shows location of Bowman Peninsula sample sites that are shown as red dots in the cross-section, and the thin black line is the 2011 grounding line (Rignot et al., 2011). The satellite image is the same as used in Fig. 1b. Cross-section: The black line is modern bedrock topography (from Bedmap 2; Fretwell et al., 2013) and blue line is the present-day ice surface profile from the Reference Elevation Model for Antarctica (Howat et al., 2018). "GL" marks position of modern (2011) grounding line. Red dots are bedrock sites that, from in situ ^{14}C dating, are inferred to have been ice-free since 6–7.5 ka; these are mapped to the nearest position on the flowline.

5.2. Comparison with other evidence for Holocene ice sheet change

In the marine geological record, grounded ice retreat from a core site near the mouth of Nantucket Inlet (PS-1423; Fig. 1) had occurred by 5.3 ± 0.3 ka (Hedges et al., 1995; Crawford et al., 1996; Fig. 3c), and subglacial lineations on the seafloor at that site provide evidence for streaming ice along Ronne Trough at that time. The in situ ^{14}C exposure ages that suggest deglaciation of the Bowman Peninsula 6–8 kyrs ago therefore concur with the timing of grounded ice retreat across the continental shelf, which was underway in the Holocene and had reached the core site PS-1423 by 5.3 ka. Based on both terrestrial and marine geological evidence, two scenarios have been suggested for LGM ice extent in the WSE; these differ over whether or not ice was grounded at the LGM in the deepest parts of palaeo-ice stream troughs that extend northwards across the continental shelf (Hillenbrand et al., 2014). The new ^{14}C exposure age data presented here do not favour one scenario over the other; since both scenarios imply that grounded ice along the Lassiter Coast had retreated close to its modern configuration between 10 and 5 ka, either would be consistent with the exposure age data.

Several regions of Antarctica have undergone hundreds of metres of ice surface lowering during the Holocene. Johnston Glacier experienced a change in ice thickness ~6–8 kyrs ago similar in abruptness and magnitude to that detected by exposure dating in both the Hudson Mountains/Pine Island Glacier in the Amundsen Sea sector (Johnson et al., 2014) and Mackay Glacier in the Ross Sea sector (Jones et al., 2015) (Fig. 6). In the southern Transantarctic Mountains, several short phases of similarly-rapid thinning are evident, but within a longer — and overall slower — trajectory of thinning that continued into the late Holocene (Spector et al., 2017; Fig. 6). In contrast, exposure ages from the Heritage Range of the Ellsworth Mountains (Hein et al., 2016) provide a less well-constrained thinning history than the other sites in Fig. 6, hence it is not possible to detect any short-lived episodes of rapid ice sheet surface lowering in that area. The Johnston Glacier data do not preclude that rapid thinning in the mid-Holocene was preceded by a slower phase of thinning immediately following the LGM (sampling at higher elevations would be required to determine this); however, in contrast to the Transantarctic Mountains data, there is no evidence that thinning — whether rapid or not — continued to the modern ice surface elevation beyond 6 ka. Thus the series of thinning histories shown in Fig. 6 demonstrates that episodes of rapid thinning resulting in a few hundred metres of surface lowering, such as that detected on the Lassiter Coast, were not uncommon in the Holocene epoch in Antarctica. Such phases of rapid upstream thinning are an expected response to phases of rapid grounding line retreat at coastal locations (e.g. Joughin et al., 2014; Jones et al., 2015). However, the causes of such retreat will vary depending on location and ice sheet dynamics. Modelling experiments in which a range of forcings can be applied to test likely influences on timing and style of deglaciation (e.g. Whitehouse et al., 2017) are needed to determine the most likely cause of the episode of rapid thinning of Johnston Glacier and to test the significance of the concurrence of mid-Holocene thinning on the Lassiter Coast with simultaneous thinning of Pine Island Glacier (Hudson Mountains) and Mackay Glacier (Fig. 6). Such model experiments are beyond the scope of the present study and, to our knowledge, none have yet been undertaken in this area by others.

5.3. Significance for GIA models

Reliable models of GIA are important for correcting estimates of ice mass loss derived from satellites such as GRACE (Bentley and Wahr, 1998). There is currently a mismatch between uplift predicted by GIA ice history models and that observed from ground-based GPS measurements in the south-east Antarctic Peninsula, particularly along the Lassiter Coast (Wolstencroft et al., 2015). This suggests that the GIA ice history models are not correct, and that grounding line retreat must have occurred later in this region than currently assumed, or that the ice sheet was thicker at the LGM. Thus an improved understanding of LGM ice sheet thickness in this region and its Holocene deglacial history from glacial-geological studies is critical for correcting the models.

The new exposure age data presented here show that at least 385 m of ice sheet lowering has occurred since 7.5 ka in the westernmost WSE, with at least 250 m of that in the mid-Holocene, 6–7.5 ka. If the rate of thinning derived from the ^{14}C age dating had been sustained for the past 20 kyrs, the LGM ice sheet would have been implausibly thick; therefore the data imply that the ice sheet could not have thinned steadily from LGM to the mid-Holocene, but that grounding line retreat occurred in a stepwise manner. This study thus provides valuable new data on Holocene deglacial history needed for improving GIA ice history models. However, it is unable to provide constraints on any late Holocene change in grounding line positions: although there is no evidence in the exposure age data for change in ice sheet thickness after 6 ka, further lowering of the ice surface below its present elevation followed by late Holocene thickening to the present configuration cannot be ruled out. Such a re-advance was invoked by

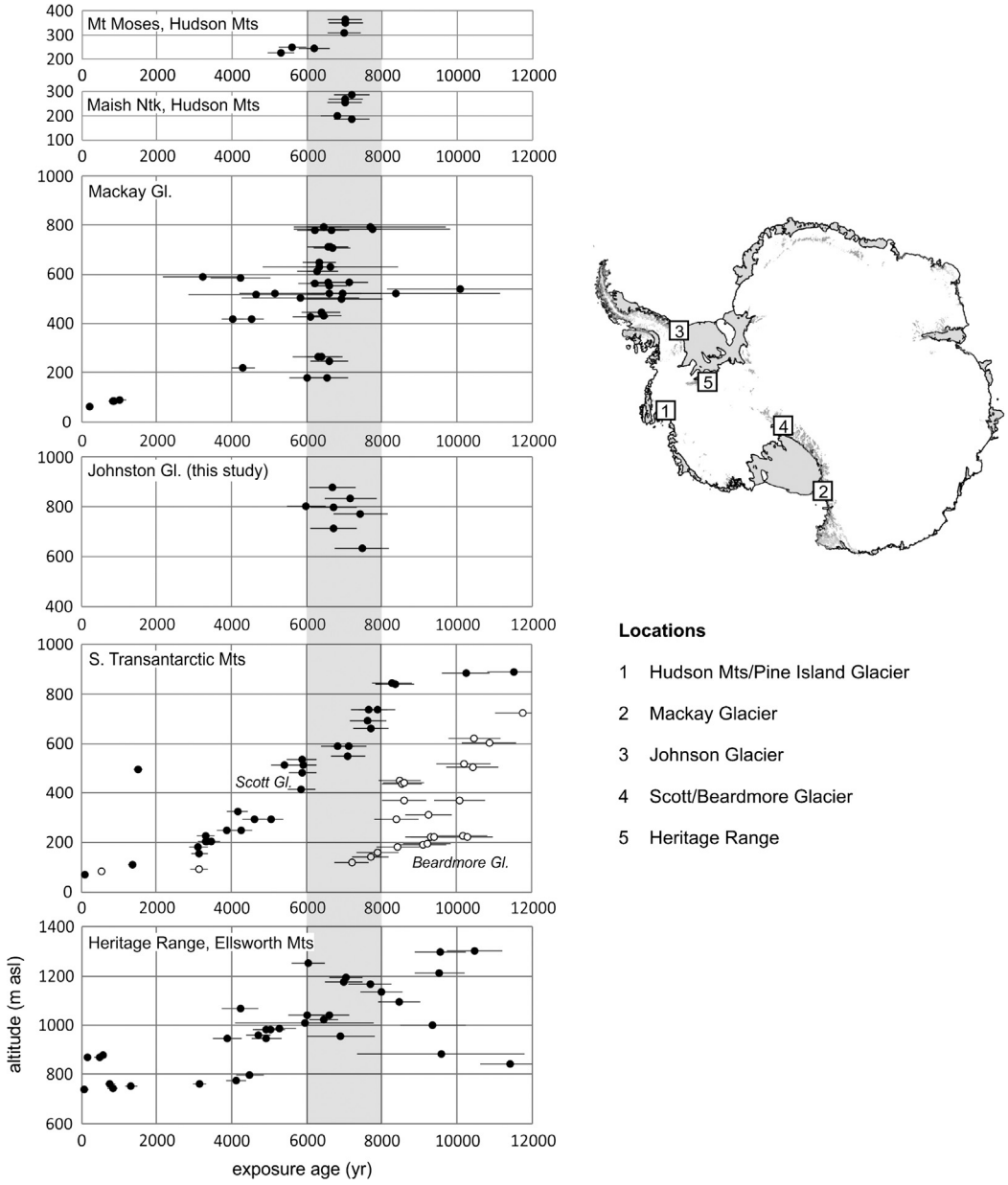

Fig. 6. Holocene thinning histories derived from exposure age dating from selected sites in Antarctica (Hudson Mountains/Pine Island Glacier, Johnson et al., 2014; Mackay Glacier, Jones et al., 2015; Johnston Glacier, this study; Scott and Beardmore Glaciers, southern Transantarctic Mountains, Spector et al., 2017; Heritage Range, Ellsworth Mountains; Hein et al., 2016). Exposure ages shown are all ^{10}Be, with the exception of Johnston Glacier where deglaciation ages were determined using in situ ^{14}C. Vertical axes are altitude (m asl) and horizontal axes are exposure age (yr). All data shown are publicly accessible on the ICE-D:Antarctica database (http://antarctica.ice-d.org). The upper five panels show locations where episodes of rapid thinning occurred at 6–8 ka (time period indicated by grey shading).

Bradley et al. (2015) to achieve a better fit of their GIA model to GPS-measured observations of uplift and to explain glaciological and geophysical evidence (Siegert et al., 2013) for reorganisation of ice flow in the south-eastern WSE in the late Holocene. In addition, recent model experiments of the West Antarctic Ice Sheet by Kingslake et al. (2018) showed that isostatic rebound caused widespread Holocene grounding line re-advance after an earlier post-LGM retreat. Although in the model this occurred during the early — rather than late — Holocene, the precise timing of re-advance is sensitive to both bed topography and forcings. Nonetheless, the new exposure age data do not preclude the possibility that some or all of the terrestrial geological record of late Holocene change lies below the modern ice surface, and therefore cosmogenic dating of rock samples obtained by subglacial bedrock drilling may be necessary to validate these interpretations.

6. Conclusions

This study presents the Holocene deglacial history of Johnston Glacier in the westernmost Weddell Sea Embayment determined from cosmogenic ^{10}Be and in situ ^{14}C exposure age dating of bedrock and erratic cobbles. Geomorphological observations combined with a mismatch between ^{10}Be and ^{14}C dates on bedrock samples — the majority yielding ^{10}Be ages in the range 100–800 ka compared with ^{14}C ages entirely of mid-Holocene age on the same samples — indicates former cover by non-erosive cold-based ice. Results from in situ ^{14}C exposure dating show that the ice sheet underwent abrupt thinning in the mid-Holocene; 250 m of surface lowering occurred in a narrow time interval (no more than 2700 years if errors are taken into account) between 6.0 ± 0.5 and 7.5 ± 0.7 ka. The results further show that between 7.5 ka and the

present, the ice sheet surface on the Bowman Peninsula has lowered by 385 m. Model experiments are needed to determine the cause of rapid mid-Holocene grounding line retreat in this area that would have triggered such abrupt deglaciation.

The deglacial history determined from the Lassiter Coast samples is consistent with evidence from the marine geological record for retreat of grounded ice close to the front of the modern Ronne Ice Shelf front adjacent to Bowman Peninsula by 5.3 kyr BP. The new data reported in the present study neither preclude nor mandate a late Holocene re-advance but show i) the occurrence of episodes of thinning more rapid than previously assumed, and ii) that terrestrial evidence for late Holocene ice sheet change in this region probably lies below the modern ice surface and would need to be accessed by subglacial bedrock drilling.

Acknowledgements

We thank BAS field assistant Roger Stilwell, and members of the 2011–12 Rothera Research Station team and BAS Air Unit for their support to JSJ during the field campaign. Technical laboratory support from Hilary Blagbrough (BAS), Roseanne Schwarz and Jean Hanley (LDEO), and staff at the NOSAMS and UC Davis Stable Isotope Facilities is also gratefully acknowledged. Andrew Fleming, Louise Ireland and Laura Gerrish (BAS) helpfully assisted with accessing REMA data used in Fig. 5, and the Polar Geospatial Center (under NSF-OPP awards 1043681 and 1559691) provided the Landsat-8 image used in Figs. 1b and 5. This work forms part of the BAS Polar Science for Planet Earth program, funded by the Natural Environment Research Council, UK. JMS acknowledges support by Columbia Climate Center and the Center for Climate and Life. We also acknowledge the financial support of NSF grant OPP-1542936 to GB and BG for in situ ^{14}C measurements. Duanne White and an anonymous reviewer are thanked for their thoughtful and constructive reviews. This is LDEO publication # 8295.

Appendix A. Supplementary material

Supplementary material related to this article can be found online at https://doi.org/10.1016/j.epsl.2019.05.002.

References

Arndt, J.E., Hillenbrand, C.-D., Grobe, H., Kuhn, G., Wacker, L., 2017. Evidence for a dynamic grounding line in outer Filchner trough, Antarctica, until the early Holocene. Geology 45, 1035–1038.

Balco, G., 2011. Contributions and unrealized potential contributions of cosmogenic-nuclide exposure dating to glacier chronology, 1990–2010. Quat. Sci. Rev. 30, 3–27.

Balco, G., Todd, C., Huybers, K., Campbell, S., Vermeulen, M., Hegland, M., Goehring, B.M., Hillebrand, T.M., 2017. Cosmogenic nuclide exposure ages from the Pensacola mountains adjacent to the foundation ice stream, Antarctica. Am. J. Sci. 316, 542–577.

Bentley, M.J., Fogwill, C.J., Kubik, P.W., Sugden, D.E., 2006. Geomorphological evidence and cosmogenic Be-10/Al-26 exposure ages for the Last Glacial Maximum and deglaciation of the Antarctic Peninsula Ice Sheet. Geol. Soc. Am. Bull. 118, 1149–1159.

Bentley, M., Fogwill, C., Le Brocq, A., Hubbard, A., Sugden, D., Dunai, T., Freeman, S., 2010. Deglacial history of the West Antarctic Ice Sheet in the Weddell Sea Embayment: constraints on past ice volume change. Geology 38, 411–414.

Bentley, M.J., Hein, A.S., Sugden, D.E., Whitehouse, P.L., Shanks, R., Xu, S., Freeman, S.P.H.T., 2017. Deglacial history of the Pensacola mountains, Antarctica from glacial geomorphology and cosmogenic nuclide surface exposure dating. Quat. Sci. Rev. 158, 58–76.

Bentley, C.R., Wahr, J.M., 1998. Satellite gravity and the mass balance of the Antarctic ice sheet. J. Glaciol. 44, 207–213.

Bradley, S.L., Hindmarsh, R.C.A., Whitehouse, P.L., Bentley, M.J., King, M.A., 2015. Low post-glacial rebound rates in the Weddell Sea due to late Holocene ice-sheet readvance. Earth Planet. Sci. Lett. 413, 79–89.

Briner, J.P., Lifton, N.A., Miller, G.H., Refsnider, K., Anderson, R., Finkel, R., 2014. Using in situ cosmogenic ^{10}Be, ^{14}C, and ^{26}Al to decipher the history of polythermal ice sheets on Baffin Island, Arctic Canada. Quat. Geochronol. 19, 4–13.

Crawford, K., Kuhn, G., Hambrey, M.J., 1996. Changes in the character of glaciomarine sedimentation in the southwestern Weddell Sea, Antarctica: evidence from the core PS1423-2. Ann. Glaciol. 22, 200–204.

DeConto, R., Pollard, D., 2016. Contribution of Antarctica to past and future sea-level rise. Nature 531, 591–597.

Fogwill, C.J., Bentley, M.J., Sugden, D.E., Kerr, A.R., Kubik, P.W., 2004. Cosmogenic nuclides Be and Al imply limited Antarctic Ice Sheet thickening and low erosion in the Shackleton range for >1 m.y. Geology 32, 265–268.

Fogwill, C.J., Turney, C.S.M., Golledge, N.R., Rood, D.H., Hippe, K., Wacker, L., Wieler, R., Rainsley, E.B., Jones, R.S., 2014. Drivers of abrupt Holocene shifts in West Antarctic ice stream direction determined from combined ice sheet modelling and geologic signatures. Antarct. Sci. 26 (6), 674–686.

Fretwell, P., Pritchard, H.D., Vaughan, D.G., Bamber, J.L., Barrand, N.E., et al., 2013. Bedmap2: improved ice bed, surface and thickness datasets for Antarctica. Cryosphere 7, 375–393.

Fütterer, D.K. (Ed.), 1987. The Expedition ANTARKTIS-IV of RV "Polarstern" 1985–1986: Report of Legs ANT-IV 3-4. Ber. Polarforsch., vol. 33.

Golledge, N.R., Menviel, L., Carter, L., Fogwill, C.J., England, M.H., Cortese, G., Levy, R.H., 2014. Antarctic contribution to meltwater pulse 1A from reduced Southern Ocean overturning. Nat. Commun. 5, 5107. https://doi.org/10.1038/ncomms6107.

Hedges, R.E.M., Housely, R.A., Bronck Ramsey, C., van Klinken, G.J., 1995. Radiocarbon dates from the Oxford AMS system: *archaeometry* datelist 19. Archaeometry 37, 195–214.

Hein, A.S., Fogwill, C.J., Sugden, D.E., Xu, S., 2011. Glacial/interglacial ice-stream stability in the Weddell Sea embayment, Antarctica. Earth Planet. Sci. Lett. 307, 211–221.

Hein, A., Fogwill, C., Sugden, D., Xu, S., 2014. Geological scatter of cosmogenic-nuclide exposure ages in the Shackleton Range, Antarctica: implications for glacial history. Quat. Geochronol. 19, 52–66.

Hein, A.S., Marrero, S.M., Woodward, J., Dunning, S.A., Winter, K., Westoby, M.J., Freeman, S.P.H.T., Shanks, R.P., Sugden, D.E., 2016. Mid-Holocene pulse of thinning in the Weddell Sea sector of the West Antarctic ice sheet. Nat. Commun. 7, 12511. https://doi.org/10.1038/ncomms12511.

Hellmer, H.H., Kauker, F., Timmermann, R., Determann, J., Rae, J., 2012. Twenty-first-century warming of a large Antarctic iceshelf cavity by a redirected coastal current. Nature 485, 225–228.

Hillenbrand, C.D., et al., 2014. Reconstruction of changes in the Weddell Sea sector of the Antarctic ice sheet since the Last Glacial Maximum. Quat. Sci. Rev. 100, 111–136. https://doi.org/10.1016/j.quascirev.2013.07.020.

Hodgson, D.A., Bentley, M.J., Schnabel, C., Cziferszky, A., Fretwell, P., Convey, P., Xu, S., 2012. Glacial geomorphology and cosmogenic ^{10}Be and ^{26}Al exposure ages in the northern Dufek Massif, Weddell Sea embayment, Antarctica. Antarct. Sci. 24 (04), 377–394.

Howat, I., Morin, P., Porter, C., Noh, M.J., 2018. The reference elevation model of Antarctica. https://doi.org/10.7910/DVN/SAIK8B. Harvard Dataverse, V1.

Johnson, J.S., Bentley, M.J., Smith, J.A., Finkel, R.C., Rood, D.H., Gohl, K., Balco, G., Larter, R.D., Schaefer, J.M., 2014. Rapid thinning of Pine Island Glacier in the early Holocene. Science 343, 999–1001. https://doi.org/10.1126/science.1247385.

Johnson, J.S., Smith, J.A., Schaefer, J.M., Young, N.E., Goehring, B.M., Hillenbrand, C.-D., Lamp, J.L., Finkel, R.C., Gohl, K., 2017. The last glaciation of Bear Peninsula, central Amundsen Sea Embayment of Antarctica: constraints on timing and duration revealed by in situ cosmogenic ^{14}C and ^{10}Be dating. Quat. Sci. Rev. 178, 77–88. https://doi.org/10.1016/j.quascirev.2017.11.003.

Jones, R.S., Mackintosh, A.N., Norton, K.P., Golledge, N.R., Fogwill, C.J., Kubik, P.W., Christl, M., Greenwood, S.L., 2015. Rapid Holocene thinning of an East Antarctic outlet glacier driven by marine ice sheet instability. Nat. Commun. 6, 8910. https://doi.org/10.1038/ncomms9910.

Joughin, I., Bamber, J.L., Scambos, T., Tulaczyk, S., Fahnestock, M., MacAyeal, D.R., 2006. Integrating satellite observations with modelling: basal shear stress of the Filcher-Ronne ice streams, Antarctica. Proc. R. Soc. Lond., Ser. A 364 (1844), 1795–1814. https://doi.org/10.1098/rsta.2006.1799.

Joughin, I., Smith, B.E., Medley, B., 2014. Marine ice sheet collapse potentially under way for the Thwaites Glacier basin, west Antarctica. Science 244, 735–738. https://doi.org/10.1126/science.1249055.

Kingslake, J., Scherer, R., Albrecht, T., Coenen, J., Powell, R., Reese, R., Stansell, N., Tulaczyk, S., Wearing, M., Whitehouse, P.L., 2018. Extensive Holocene West Antarctic Ice Sheet retreat and rebound driven re-advance. Nature 558, 430–434.

Maris, M.N.A., van Wessem, J.M., van de Berg, W.J., de Boer, B., Oerlemans, J., 2015. A model study of the effect of climate and sea-level change on the evolution of the Antarctic Ice Sheet from The Last Glacial Maximum to 2100. Clim. Dyn. 45, 837–851.

Pollard, D., Chang, W., Haran, M., Applegate, P., DeConto, R., 2016. Large ensemble modeling of the last deglacial retreat of the West Antarctic Ice Sheet: comparison of simple and advanced statistical techniques. Geosci. Model Dev. 9, 1697–1723.

Pollard, D., Gomez, N., DeConto, R.M., 2017. Variations of the Antarctic Ice Sheet in a coupled ice sheet-Earth-sea level model: sensitivity to viscoelastic Earth properties. J. Geophys. Res. 122, 2124–2138.

Rignot, E., Mouginot, J., Scheuchl, B., 2011. Antarctic grounding line mapping from differential satellite radar interferometry. Geophys. Res. Lett. 38, L10504.

Ritz, C., Edwards, T.L., Durand, G., Payne, A.J., Peyaud, V., Hindmarsh, R.C.A., 2015. Potential sea-level rise from Antarctic ice-sheet instability constrained by observations. Nature 528, 115–118.

Siegert, M., Ross, N., Corr, H., Kingslake, J., Hindmarsh, R., 2013. Late Holocene ice-flow reconfiguration in the Weddell Sea sector of West Antarctica. Quat. Sci. Rev. 78, 98–107. https://doi.org/10.1016/j.quascirev.2013.08.003.

Spector, P., Stone, J.O., Cowdery, S.G., Hall, B., Conway, H., Bromley, G., 2017. Rapid early-Holocene deglaciation in the Ross Sea, Antarctica. Geophys. Res. Lett. 44. https://doi.org/10.1002/2017GL074216.

Spector, P., Stone, J., Pollard, D., Hillebrand, T., Lewis, C., Gombiner, J., 2018. West Antarctic sites for subglacial drilling to test for past ice-sheet collapse. Cryosphere 12, 2741–2757.

Stolldorf, T., Schenke, H.-W., Anderson, J.B., 2012. LGM ice sheet extent in the Weddell Sea: evidence for diachronous behavior of Antarctic Ice Sheets. Quat. Sci. Rev. 48, 20–31.

Stone, J.O., Balco, G., Sugden, D., Caffee, M., Sass III, L., Cowdery, S., Siddoway, C., 2003. Holocene deglaciation of Marie Byrd Land, West Antarctica. Science 299, 99–102.

Sugden, D.E., Balco, G., Cowdery, S.G., Stone, J.O., Sass III, L.C., 2005. Selective glacial erosion and weathering zones in the coastal mountains of Marie Byrd Land, Antarctica. Geomorphology 67 (3–4), 317–334. https://doi.org/10.1016/j.geomorph.2004.10.007.

Vennum, W.R., Rowley, P.D., 1986. Reconnaissance geochemistry of the Lassiter Coast Intrusive Suite, southern Antarctic Peninsula. Geol. Soc. Am. Bull. 97, 1521–1533.

Whitehouse, P.L., Bentley, M.J., Le Brocq, A.M., 2012. A deglacial model for Antarctica: geological constraints and glaciological modelling as a basis for a new model of Antarctic glacial isostatic adjustment. Quat. Sci. Rev. 32, 1–24. https://doi.org/10.1016/j.quascirev.2011.11.016.

Whitehouse, P.L., Bentley, M.J., Vieli, A., Jamieson, S.S.R., Hein, A., Sugden, D., 2017. Controls on Last Glacial Maximum ice extent in the Weddell Sea embayment, Antarctica. J. Geophys. Res. 122, 371–397. https://doi.org/10.1002/2016JF004121.

Wolstencroft, M., King, M.A., Whitehouse, P.L., Bentley, M.J., Nield, G.A., King, E.C., McMillan, M., Shepherd, A., Barletta, V., Bordoni, A., Riva, R.E.M., Didova, O., Gunter, B.C., 2015. Uplift rates from a new high-density GPS network in Palmer Land indicate significant late Holocene ice loss in the southwestern Weddell Sea. Geophys. J. Int. 203, 737–754.

Wright, A.P., LeBrocq, A.M., Cornford, S.L., Bingham, R.G., Corr, H.J.F., Ferraccioli, F., Jordan, T.A., Payne, A.J., Rippin, D.M., Ross, N., Siegert, M.J., 2014. Sensitivity of the Weddell Sea sector ice streams to sub-shelf melting and surface accumulation. Cryosphere 8, 2119–2134.

Young, N.E., Lamp, J., Koffman, T., Briner, J.P., Schaefer, J., Gjermundsen, E.F., Linge, H., Zimmerman, S., Guilderson, T.P., Fabel, D., Hormes, A., 2018. Deglaciation of coastal south-western Spitsbergen dated with *in situ* cosmogenic ^{10}Be and ^{14}C measurements. J. Quat. Sci. 33 (7), 763–776. https://doi.org/10.1002/jqs.3058.